International Journal of General Medicine

Dovepress
open access to scientific and medical research

Open Access Full Text Article

CLINICAL TRIAL REPORT

Alterations of White Matter Connectivity in Adults with Essential Hypertension

Weijie Chen[1,2,*], Simin Deng[3,*], Huali Jiang[2,*], Heng Li[2], Yu Zhao[2], Yiqiang Yuan[4]

[1]Department of Cardiology, The Second School of Clinical Medicine, Southern Medical University, Guangdong, People's Republic of China; [2]Department of Cardiology, Dongguan Tung Wah Hospital, Guangdong, People's Republic of China; [3]Research Center, Dongguan Eighth People's Hospital, Guangdong, People's Republic of China; [4]Department of Cardiology, The Second School of Clinical Medicine, Southern Medical University, The Seventh People's Hospital of Zhengzhou, Henan, People's Republic of China

*These authors contributed equally to this work

Correspondence: Yiqiang Yuan, Department of Cardiology, The Second School of Clinical Medicine, Southern Medical University, The Seventh People's Hospital of Zhengzhou, No. 17 Jingnan 5th Road, Zhengzhou Economic and Technological Development Zone, Zhengzhou, Henan, People's Republic of China, Tel +86-0371-61205666, Email zzqyyuanyiqiang@126.com

Purpose: To explore the topology of the white matter network in individuals with essential hypertension by graph theory.

Patients and Methods: T1-weighted image and diffusion tensor imaging (DTI) data from 43 patients diagnosed with essential hypertension (EHT) and 33 individuals with normotension (healthy controls, HCs) were incorporated in this cross-sectional study. Furthermore, structural networks were constructed by graph theory to calculate whole brain network characteristics and intracerebral node characteristics.

Results: Both EHT and HC groups displayed small-worldness in their structural networks. The area under the curve (AUC) of the small-worldness coefficient (σ) was higher in the EHT group compared to the HC group, whereas the AUC of assortativity was lower in the EHT group in contrast to the HC group. The nodal clustering coefficient (CP) and local efficiency (Eloc) of the EHT group decreased in the right dorsolateral superior frontal gyrus and the left medial superior frontal gyrus. These values increased in the left anterior cingulate and paracingulate gyrus. Furthermore, weight and body mass index (BMI) were positively correlated with σ.

Conclusion: The EHT group showed brain network separation and integration dysfunction. Weight and BMI were positively correlated with σ. The data acquired in this investigation implied that altered structural connectivity in the prefrontal region may be a potential neuroimaging marker in EHT patients.

Keywords: DTI, EHT, graph theory, whole brain network characteristics, intracerebral node characteristics

Introduction

The global aging population has led to the emergence of dementia (DA) as a significant healthcare concern. In 2019, approximately 55 million people were diagnosed with dementia, a number estimated to rise to 78 million by 2030 and 139 million by 2050.[1] Dementia places a substantial economic burden on patients, families, and societies. Global spending on DA reached $1.3 trillion in 2019 and is projected to double, potentially reaching as high as $2.8 trillion by 2030.[2] The two common types of DA include Alzheimer's disease (AD), responsible for 60–80% of cases, and vascular dementia (VD), caused by cerebrovascular disease which accounts for 5–10% of cases.[3] Hypertension is a critical modifiable risk factor for AD, VD, and mild cognitive impairment.[4–8] It not only causes acute and chronic damage to the brain by directly influencing the brain structures and microvasculature, which accelerates brain atrophy, but also participates in the neuroinflammatory processes that lead to the development of DA.[9] Moreover, it can also increase the incidence of DA through other organ damage, such as chronic kidney disease and heart failure.[10] Studying the early effects of hypertension on the brain can contribute to preventing, delaying, or treating cognitive impairment and dementia.

Diffusion tensor imaging (DTI) is an approach that utilizes diffusion-sensitive gradient pulses to amplify the diffusion effect of water molecules. It is used to study the differences in the diffusive movement of water molecules in different

Received: 3 November 2023
Accepted: 19 January 2024
Published: 31 January 2024

tissues. Moreover, DTI allows for the observation of the structural integrity and connectivity of tissues. Studies on AD using DTI revealed that the microstructural changes in neurons precede the macroscopic atrophic alterations in AD pathogenesis,[11] therefore, DTI may be helpful for early diagnosis. Based on the quantitative studies of DTI diffusion parameters, Hannawi et al[12] showed that the fractional anisotropy (FA) of the right cingulate gyrus and left stria terminalis in hypertensive patients was significantly reduced. Additionally, they found a significant correlation between the systolic blood pressure (BP) values and local FA in the left superior longitudinal fasciculus. Hannesdottir et al[13] found that the mean FA values in treated hypertensive patients were lower than in untreated hypertensive patients. The study by Chetouani et al[14] observed a link between changes in the white matter structure and metabolic activity in cortical areas of the brain affected by AD. This association was identified in elderly individuals with hypertension who were experiencing subjective memory impairment.

Lorenzo Carnevale et al[15] found that patients with essential hypertension (EHT) exhibited altered connectivity in the dorsal attention network and sensorimotor network, the dorsal attention network and visual network, as well as the dorsal attention network and frontoparietal network, compared to patients with normotension. In EHT patients, alterations in brain functional connectivity networks were observed. These alterations were similar to those seen in patients with dementia, including cognitive dysfunction and altered microstructural integrity of the brain. The association between the FA of the superior longitudinal fasciculus and the dorsal attention network and default mode network (DMN), as well as the association between Montreal Cognitive Assessment scores and widespread functional connectivity networks, was examined. The results showed that patients with EHT had altered connectivity in brain functional networks, similar to the cognitive dysfunction and changes in brain microstructure observed in dementia patients. However, the study was limited to the quantification of diffusion parameters in DTI and the construction of resting-state functional magnetic resonance imaging (MRI) networks, without an in-depth investigation of the white matter structural networks.

Based on the above information, we hypothesized that patients with EHT exhibited changes in whole brain network characteristics and intracerebral node characteristics in the structural network prior to the onset of cognitive decline. To validate the aforementioned hypothesis, this study included 43 patients with EHT and 33 individuals with normotension (healthy controls, HCs). T1-weighted image and DTI data were acquired. Based on FA, deterministic fiber tracking was utilized to construct the structural network. Graph theory analysis was then used to investigate the whole brain network characteristics and intracerebral node characteristics of both groups.

Patients and Methods

Study Subjects

This study was conducted in the Department of Cardiology, Dongguan Tung Wah Hospital. It was performed according to the principles of the Declaration of Helsinki and obtained approval from the institutional ethics committee (Dongguan Tung Wah Hospital medical ethics committee 2021-KY-034), was registered with the Chinese Clinical Trial Registry (Registration Number: ChiCTR2100053166), and received informed consent from each study participant. This study included 43 patients with EHT and 33 HCs with normotension.

Inclusion criteria for the EHT group: 1) Hypertension was diagnosed based on office BP. Office BP measurements should align with the recommendations outlined in the 2020 International Society of Hypertension global hypertension practice guidelines.[16] Three measurements were taken at each visit with a 1-minute interval between them, and the average of the last two measurements was calculated. Hypertension was diagnosed at systolic BP $\geq$ 140 mmHg and/or diastolic BP $\geq$ 90 mmHg during 2–3 office visits. BP was measured in the sitting position by an oscillometric device (Omron HBP-1300, Kyoto, Japan) with an appropriately sized cuff on the dominant arm. Patients with a history of hypertension and those currently receiving treatment with antihypertensive medications were also diagnosed with hypertension; 2) Mini-Mental State Examination (MMSE) score between 24 and 30 (inclusive), an unauthorized version of the Chinese MMSE was used by the study team without permission and has been rectified with PAR; 3) Clinical Dementia Rating Scale (CDR) score of 0.

Inclusion criteria for the HC group: 1) Systolic BP < 140 mmHg and diastolic BP < 90 mmHg, no previous diagnosis of hypertension and treatment with antihypertensive drugs; 2) MMSE and CDR scores were the same as the EHT group.

Exclusion criteria: 1) Cognitive abnormalities, such as dementia, any other diagnosed neurological or psychiatric diseases, and the use of medications that may impact cognitive function; 2) Presence of MRI abnormalities, such as strokes, seizures, or Parkinson's disease; 3) Secondary hypertension; 4) Presence of other diseases, such as severe medical conditions like heart failure, renal insufficiency, hepatic insufficiency, atrial fibrillation, tumors, hematologic disorders, chronic lung infections, diabetes, etc.

MRI Data Acquisition and Pre-Processing

The structural MRI and DTI data of all subjects was acquired at Dongguan Tung Wah Hospital by employing a 3 Tesla MRI system (Magnetom Skyra; Siemens Healthcare, Erlangen, Germany). Structural MRI was performed by using T1-weighted images with 3D magnetization prepared rapid gradient echo (MPRAGE) to provide an anatomical reference for the DTI analysis (Figure 1). Additionally, axial T2-weighted imaging, diffusion-weighted imaging (DWI) sequences, and fluid attenuated inversion recovery (FLAIR) sequences were acquired to evaluate the absence of white matter lesions, cerebral hemorrhage, or ischemic lesions, brain tumors, and other abnormalities. The diagnoses were made by the same radiologist. Moreover, DTI was carried out by utilizing echo planar imaging (EPI) sequences (Figure 1). The participants were scanned while lying in a supine position with their heads fixed using foam padding to minimize head motion. Any scans with head motion exceeding or equal to 2° and 2mm were excluded. The scanning parameters for DTI were as follows: repetition time of 3700 ms; echo time of 92 ms; 25 slices; 90° excitation and 180° refocusing radio frequency (RF) pulse; spatial resolution of 1.7*1.7*4.0 mm^3; 12 zero-weighted images (b = 0 s/mm^2); 60 nonlinear diffusion-weighted directions (b = 1000 s/mm^2); acquisition matrix of 128*128; field of view (FOV) of 220*220.

PANDA (Pipeline for Analyzing Brain Diffusion Images, http://www.nitrc.org/projects/panda/) software[17] was used for preprocessing DTI data. The preprocessing steps are as follows: 1) Convert DICOM data to NIFTI format. 2) Perform skull-stripping on the B0 image. 3) Register the diffusion-weighted images with the B0 image using affine transformation, correcting for the eddy current distortions and head motion during the scan. 4) Calculate the FA values using the dtifit command of FSL.

Construction and Analysis of Brain Networks

Definition of network nodes: The brain was divided into 90 brain regions using the automated anatomical labeling (AAL90) template. Each brain region was considered a node in the brain network. Each FA image was aligned with the corresponding T1-weighted image through affine transformation. Subsequently, the transformed T1-weighted images were aligned onto the International Consortium for Brain Mapping (ICBM152) template through non-linear registration; the inverse transformation T^{-1} was obtained; then, the inverse transformation T^{-1} was applied to the selected AAL90 template to obtain a partition of 90 brain regions based on this template.

Definition of network edges: Brain networks were constructed using the deterministic fiber tracking method. Edges represented the white matter fiber bundles connecting two nodes, with FA values playing an important role in evaluating white matter fiber integrity. Additionally, selecting the average FA value was easier to obtain compared to selecting fiber

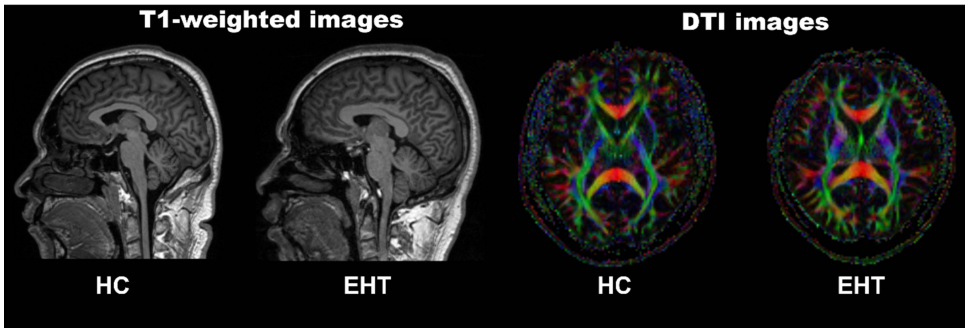

Figure 1 The image shows T1-weighted and DTI images of the HC group and the EHT group. The T1-weighted images were acquired using the MPRAGE sequence, while the DTI images were acquired using the EPI sequence.

Abbreviations: DTI, diffusion tensor imaging; HC, healthy control; EHT, essential hypertension; MPRAGE, magnetization prepared rapid gradient echo; EPI, echo planar imaging.

bundles as network edges.[18] Therefore, the average FA value between two nodes was defined as the network edges.[19] If the crossing angle between two consecutive moving directions was greater than 45 degrees or if FA exceeded the threshold range (default 0.2–1), tracking was terminated.[20] PANDA was employed to compute the 90×90 matrix weighted by FA, and the resultant matrix was saved as a MATLAB (MathWorks, Natick, MA, USA) data file for subsequent graph theory analysis.

Network Properties

Network analysis was performed using GRETNA toolbox.[21] Since the structural network of the white matter of the brain is a sparse network itself, with the number of connection edges accounting for about 20% of the total connections, threshold processing was typically unnecessary in structural network analysis. Instead, network attribute analysis was directly based on the weighted network. The following metrics were calculated on whole brain network characteristics:[22] 1) small-world properties: small-worldness coefficient (σ), clustering coefficient (CP), shortest path length (LP), normalized clustering coefficients (γ) and normalized characteristic path length (λ); 2) efficiency: global efficiency (Eg) and local efficiency (Eloc); 3) assortativity. The following metrics were calculated on intracerebral node characteristics:[22] 1) nodal CP; 2) nodal LP; 3) nodal Eg; 4) nodal Eloc; 5) nodal degree centrality (DC); and 6) nodal betweenness centrality (BC).

Statistical Analysis

Statistical analysis of the demographic and clinical data of the EHT and HC groups was performed using the SPSS 26.0 statistical analysis software (SPSS Inc., Chicago, IL, USA). Independent samples *t*-test was employed for continuous variables, whereas the chi-square (X^2) test was utilized for dichotomous variables. When $p < 0.05$, the difference was considered statistically significant. The Global and Nodal Metric Comparison module of GRETNA was utilized to perform a two-sample *t*-test on network properties. For results showing significant differences, post hoc multiple comparison correction using the FDR correction method was performed with the threshold set at $p < 0.05$.

Results

Demographic Data

Table 1 summarizes the differences in the demographic, clinical indicators, and neuropsychology between the two groups of study subjects. The EHT group showed significantly higher values than the HC group in terms of weight, body mass index (BMI), systolic BP, diastolic BP, left atrial diameter (LAD), interventricular septal thickness at end-diastole (IVSd), and left ventricular posterior wall thickness at end-diastole (LVPWd), with $p < 0.05$.

Global Properties Analysis

When performing inter-group statistical comparisons, we utilized the Area Under Curve (AUC) as the independent variable. Figures 2 and 3, and Table 2 illustrate the comparison of global property analysis results between the EHT and HC groups. Both groups demonstrated small-world properties in the functional network. The AUC value of σ in the EHT group was higher than that in the HC group ($p < 0.05$, Figure 2), while the AUC value of assortativity in the EHT group was lower than that in the HC group ($p < 0.05$, Figure 3). However, the results did not reach statistical significance in the remaining indicators of small-world properties, global efficiency, and local efficiency ($p > 0.05$, Table 2).

Local Properties Analysis

In the EHT group, nodal CP and nodal Eloc decreased in the right dorsolateral superior frontal gyrus and left medial superior frontal gyrus, while they increased in the left anterior cingulate and paracingulate gyrus ($p < 0.05$; Figure 4, Table 3).

Table 1 Demographic Differences Between the EHT and HC Groups

Demographic	EHT (n=43)	HC (n=33)	*p* value
Age (years)	45.79 ± 11.41	48.18 ± 8.60	0.301
Gender (M/F)	30/13	19/14	0.271
Education level (years)	12.07 ± 3.45	10.97 ± 3.05	0.152
Height (cm)	167.35 ± 7.19	163.88 ± 8.07	0.052
Weight (kg)	73.97 ± 13.84	65.39 ± 10.41	0.004*
BMI (kg/m^2)	26.25 ± 3.73	24.31 ± 3.20	0.020*
Smoking history	12	10	0.819
Systolic blood pressure (mmHg)	141.86 ± 14.61	114.12 ± 6.99	0.000*
Diastolic blood pressure (mmHg)	89.51 ± 8.48	69.42 ± 5.12	0.000*
Creatinine (umol/L)	79.51 ± 17.20	72.95 ± 16.08	0.094
LDL-C (mmol/L)	3.12 ± 0.77	3.05 ± 0.76	0.685
HDL-C (mmol/L)	1.12 ± 0.30	1.13 ± 0.42	0.944
TG (mmol/L)	1.79 ± 1.24	1.81 ± 1.01	0.955
ESR (mm/h)	14.35 ± 9.74	11.85 ± 7.50	0.210
LAD (mm)	32.51 ± 4.42	30.18 ± 2.71	0.006*
LVDd (mm)	45.30 ± 3.78	45.52 ± 2.74	0.777
IVSd (mm)	10.93 ± 1.35	9.58 ± 0.90	0.000*
LVPWd (mm)	10.58 ± 1.22	9.39 ± 0.86	0.000*
LVEF (%)	65.35 ± 4.05	66.73 ± 4.13	0.149
MMSE	29.02 ± 1.28	28.96 ± 1.42	0.864

Notes: The data is described as mean ± SD. *$p < 0.05$ indicates significant differences between the groups.
Abbreviations: M, male; F, female; BMI, body mass Index; LDL-C, low-density lipoprotein cholesterol; HDL-C, high-density lipoprotein cholesterol; TG, triglycerides; ESR, erythrocyte sedimentation rate; LAD, left atrial diameter; LVDd, left ventricular diameter at end-diastole; IVSd, interventricular septal thickness at end-diastole; LVPWd, left ventricular posterior wall thickness at end-diastole; LVEF, left ventricular ejection fraction; MMSE, Mini-Mental State Examination.

Correlation Analysis Between the Differences in the Topological Properties of the Network and the Demographic Data

Correlation analysis was performed to examine the relationship between the significantly different network indicators in the two groups and the demographic of the patients. After controlling for gender and age, the correlation analysis revealed that weight and BMI were positively correlated with σ (r = 0.2312, $p = 0.0445$; r = 0.2276, $p = 0.0481$; Figure 5). No significant correlation was found between topological features and systolic BP, diastolic BP, IVSd, and LVPWd.

Discussion

This study utilized DTI combined with graph theory analysis to investigate the topological properties of the brain white matter structural network in adult EHT patients. The outcomes demonstrated that (1) The EHT group showed a significant increase in the AUC value of σ, while the AUC value of assortativity decreased; (2) Changes of nodal CP and nodal Eloc in the EHT group primarily occurred in the prefrontal lobe; (3) Weight and BMI were positively

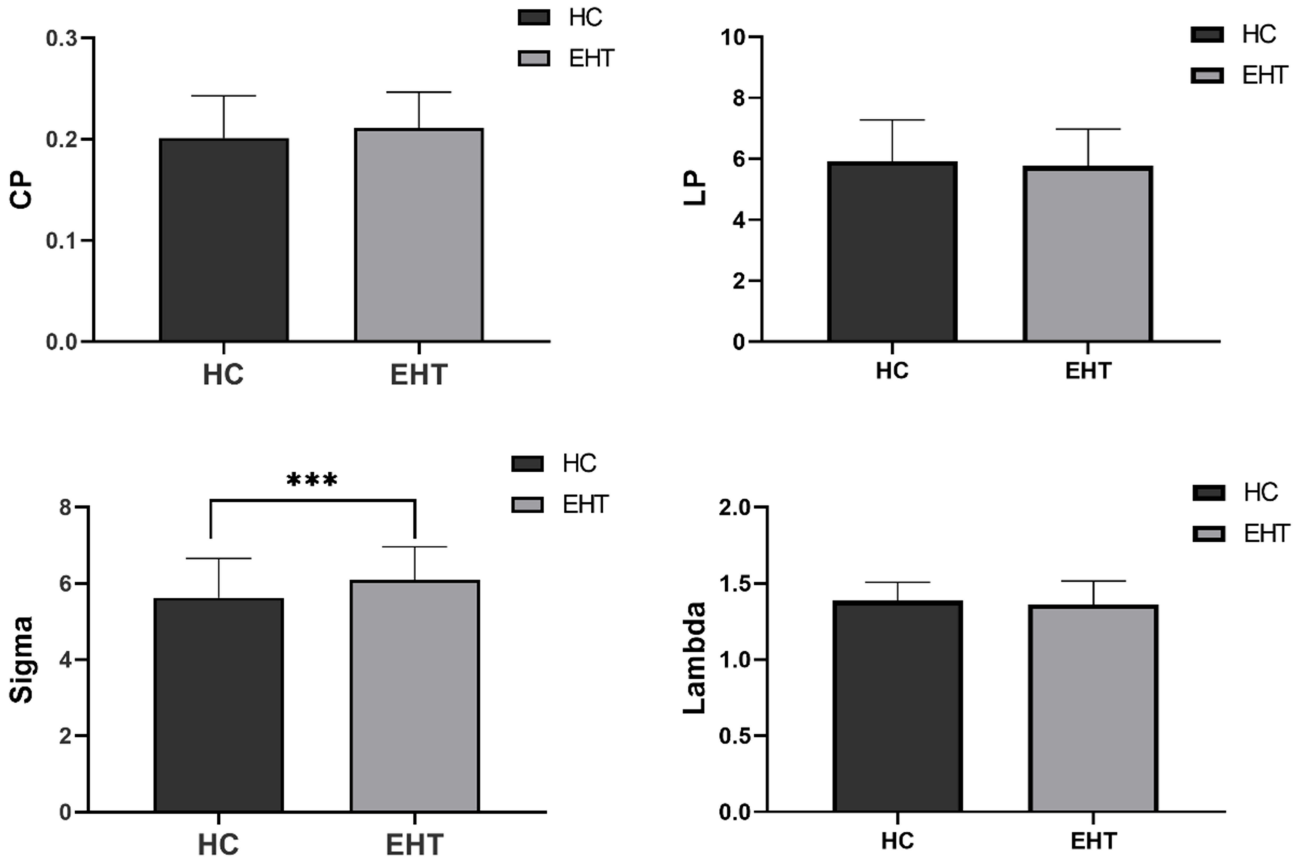

Figure 2 The global metrics of the brain between the HC and EHT group. The sigma values of the EHT group showed a significant increase compared to those of the HC group ($p < 0.05$). However, there were no significant differences observed in the CP, LP, and lambda between the two groups. *** indicates significant differences between the groups.

Abbreviations: CP, clustering coefficient; LP, shortest path length; Sigma, small-worldness coefficient; Lambda, normalized characteristic path length; HC, healthy control; EHT, essential hypertension.

correlated with σ. The findings of this study broaden our understanding of the neurophysiological mechanisms involved in EHT from the perspective of the brain white matter structural network.

Small-world network is a type of network model that lies between regular network and random network, exhibiting high CP and low LP. The σ can be defined using CP and LP: $\gamma > 1$, where γ is the ratio of the real networks' CP value to the average CP value of 500 random networks; $\lambda \approx 1$, where λ is the ratio of the real network's LP value to the average LP value of 500 random networks; and $\sigma = \gamma / \lambda$. Small-world properties are attributed to networks when $\sigma > 1$.[23,24] Our study findings revealed that both the EHT and HC groups exhibited small-worldness in networks with the EHT group demonstrating higher AUC values of σ compared to the HC group. The study indicated that the EHT group displayed more significant characteristics of high CP and low LP values. The CP reflected the local information processing capability of the brain networks, with higher CP values suggesting stronger local information processing capability. On the other hand, the LP reflected the global information integration capability of the brain networks, with lower LP values indicating stronger global information integration capability.[25]

The AUC of assortativity is lower in the EHT group compared to the HC group, implying a reduction in mutual connections among neighboring nodes. Therefore, we hypothesized a decrease in short-range connections between adjacent brain regions and an increase in long-range connections between distant brain regions in EHT patients. The balance between local specialization and global integration of the brain network was disrupted, leading to a decrease in network segregation and an increase in compensatory integration capability. Carnevale et al[15] did not detect any alterations in the whole brain network characteristics of hypertensive patients using graph theory analysis of functional MRI (fMRI). The inconsistent results could be attributed to several reasons. Firstly, variations in the types of

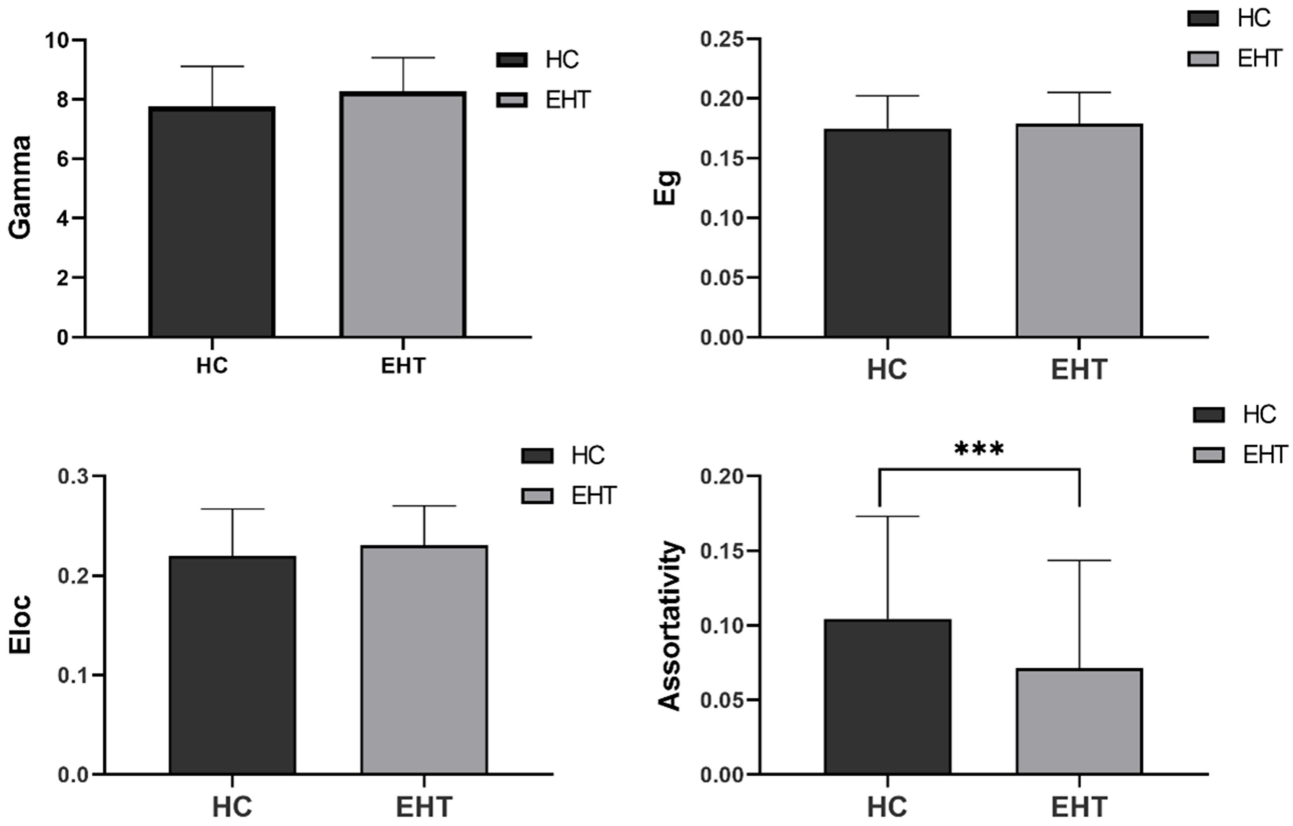

Figure 3 The assortativity of the EHT group exhibited a significant decrease in comparison to the HC group ($p < 0.05$). There were no significant variations observed in the gamma, Eg, and Eloc between the two groups. *** indicates significant differences between the groups.
Abbreviations: Gamma, normalized clustering coefficients; Eg, global efficiency; Eloc, local efficiency; HC, healthy control; EHT, essential hypertension.

hypertension within the participants might account for the disparity. This study selected individuals with EHT, while Carnevale et al incorporated patients with hypertension without excluding cases of secondary hypertension. Secondly, there were variations in the research techniques utilized, as Carnevale et al employed resting state-fMRI for their

Table 2 Global Graph Metrics of Brain Connectome Differences Between the EHT and HC Groups

Global Properties	EHT (43)	HC (33)	*F* value	*p* value
CP	0.2114 ± 0.3512	0.2013 ± 0.4190	1.139	0.256
LP	5.7588 ± 1.2196	5.9162 ± 1.3617	0.226	0.598
λ	1.3631 ± 0.1529	1.3863 ± 0.1206	0.003	0.477
γ	8.2656 ± 1.1397	7.7522 ± 1.3577	1.735	0.077
σ	6.0956 ± 0.8675	5.6230 ± 1.0353	1.183	0.034*
Eg	0.1789 ± 0.0263	0.1749 ± 0.0272	0.032	0.514
Eloc	0.2306 ± 0.0394	0.2177 ± 0.0455	1.176	0.293
Assortativity	0.0712 ± 0.0724	0.1043 ± 0.06870	0.121	0.0447*

Notes: The data is described as mean ± SD. *$p < 0.05$ indicates significant differences between the groups. The analysis of variance test was employed to obtain the F value.
Abbreviations: CP, clustering coefficient; LP, shortest path length; λ, normalized characteristic path length; γ, normalized clustering coefficients; σ, small-worldness; Eg, global efficiency; Eloc, local efficiency; HC, healthy control; EHT, essential hypertension.

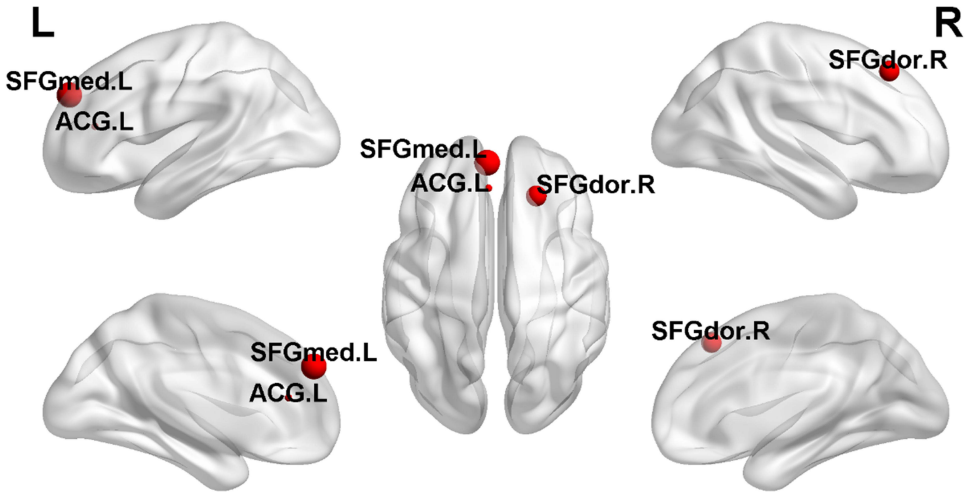

Figure 4 Predominant nodes with significant differences in node graph metrics.
Abbreviations: SFGdor.R, superior frontal gyrus, dorsolateral, right; SFGmed.L, superior frontal gyrus, medial, left; ACG.L, anterior cingulate and paracingulate gyrus, left.

investigation, whereas this study utilized DTI. In hypertensive patients, brain white matter damage tends to occur earlier and appears to be more severe.[26] Individuals with hypertension exhibited a higher incidence and a broader extent of white matter damage in the brain compared to normotensive individuals.[27] Treated hypertensive patients had a lower prevalence of brain white matter damage.[27] Appropriate antihypertensive treatment can effectively prevent the development and slow the progression of white matter damage in the brain.[28,29] The presence of brain white matter damage in asymptomatic hypertensive individuals serves as a silent marker of early brain injury.[30] After analyzing the DTI of the brain's white matter structural network, it was found that compensatory changes take place in the structural network during the early stages of hypertension in asymptomatic patients. Interestingly, similar changes in the structural network were also observed in patients with cognitive impairment.[31]

Correlation analysis controlling for gender and age revealed that weight (r = 0.2312, p = 0.0445) and BMI (r = 0.2276, p = 0.0481) had a positive correlation with σ. Overweight and obesity are associated with an increased risk of hypertension.[32] BMI is one of the most commonly used weight measurement indicators in medical research.[33] Hence, a strong association exists between BMI and BP.[34] Obesity can lead to elevated BP by increasing cardiac output, activating the renin-angiotensin-aldosterone system, and promoting inflammation.[35] Penetrating cerebral arteries plays a crucial role by supplying oxygen and nutrients to the white matter regions, maintaining normal brain tissue function. Hypertension is likely to damage the penetrating cerebral arteries, leading to white matter injury and alterations in the structural network of white matter.[13] Sabisz et al[36] revealed no significant correlation between DTI diffusion parameters

Table 3 Brain Regions with Significant Nodal Clustering Coefficient and Nodal Local Efficiency Variations Between the Groups

AAL Number	Corresponding Brain Regions	Anatomical Classification	CP		Eloc	
			p	*F*	*p*	*F*
4	Frontal_Sup_R	Prefrontal	0.0004	3.6882	0.0004	3.6882
23	Frontal_Sup_Medial_L	Prefrontal	0.0319	2.1873	0.0319	2.1873
31	Cingulum_Ant_L	Prefrontal	0.0214	−2.3506	0.0214	−2.3506

Notes: $p < 0.05$ indicates significant differences between the groups. The F value was obtained by performing the analysis of the variance test.
Abbreviations: AAL, automated anatomical labeling; CP, clustering coefficient; Eloc, local efficiency; Frontal_Sup_R, superior frontal gyrus, dorsolateral, right; Frontal_Sup_Medial_L, superior frontal gyrus, medial, left; Cingulum_Ant_L, anterior cingulate and paracingulate gyrus, left.

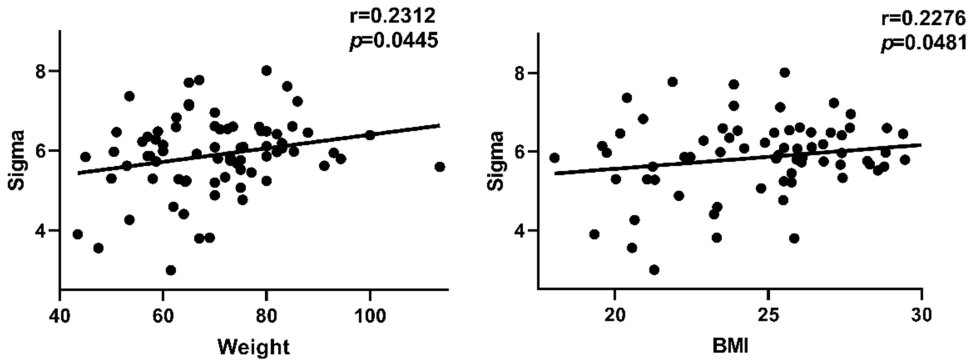

Figure 5 Relationship between global graph metrics and demographic characteristics. Sigma was positively correlated with both weight (r = 0.2312, p = 0.0445) and BMI (r = 0.2276, p = 0.0481).
Abbreviations: Sigma, small-worldness coefficient; BMI, body mass index.

and BMI in hypertension patients, but our study revealed that patients with higher weight and BMI were more likely to exhibit compensatory changes in σ.

In terms of intracerebral node characteristics, nodal CP and nodal Eloc in the EHT group showed a decrease in the right dorsolateral superior frontal gyrus and left medial superior frontal gyrus, along with an increase in the left anterior cingulate and paracingulate gyrus. The aforementioned brain regions all belong to the prefrontal cortex. A notable association was observed between the prefrontal cortex and hypertension, and elevated blood pressure was usually associated with hemodynamic abnormalities in the prefrontal cortex.[37] The findings were consistent with the data acquired by Raz et al[38] indicating that the prefrontal cortex is a particularly sensitive region to blood pressure elevation. Moreover, Bu et al[39] observed decreased functional connectivity within the prefrontal cortex in hypertensive patients using fMRI. The prefrontal cortex is one of the most crucial brain regions in the human body, mainly involved in cognition, memory, and emotional regulation.[40] Wong et al[41] demonstrated the involvement of the prefrontal cortex in the regulation of the cardiovascular system and the activation of prefrontal and subcortical areas during cognitive and emotional tasks. Wang et al[42] found that mental stress alters cardiac performance through the autonomic nervous system associated with prefrontal activity. Furthermore, Norton et al[43] observed a negative correlation between prefrontal cortex activation and heart rate acceleration.

This study found a decrease in nodal CP and nodal Eloc in the right dorsolateral superior frontal gyrus and left medial superior frontal gyrus and an increase in the left anterior cingulate and paracingulate gyrus. The superior frontal gyrus is located in the upper region of the prefrontal cortex and is involved in various neural functions. The dorsolateral superior frontal gyrus is connected to the middle frontal gyrus and inferior frontal gyrus through arcuate fibers, serving as a key node in the DMN and cognitive control network.[44] The medial superior frontal gyrus is connected to the anterior and middle cingulate cortex via the cingulate. The anterior cingulate cortex is the core node of the DMN and was found to be closely associated with the DMN and involved in its task processing.[44] The anterior cingulate and paracingulate gyrus are integral components of the DMN, a default activity network of the human brain that operates in the absence of any external stimuli. The DMN consists of two main parts: the anterior part participates in self-related psychological stimuli, while the posterior part is involved in memory-related processes.[45] The executive network is involved in goal-directed activities characterized by cognitive control and working memory.[46] Nodal CP and nodal Eloc reflect the local information processing capacity of the functional brain networks and to some extent their ability to defend against random attacks. A decrease in CP and Eloc indicates a weakened local information processing capacity of the brain network and a decrease in the ability of the network to resist attacks. Furthermore, altered connectivity in the structural brain network was observed in patients with EHT, which is similar to the cognitive dysfunction and altered micro-structural integrity in patients with dementia.[47,48]

Our study still has some limitations. Firstly, the selection of a reliable DTI analysis method that can reproduce known anatomical structures is controversial, and its results depend heavily on data quality, selected algorithms, and parameter settings.[49] Deterministic fiber tractography is a fast method, but it is characterized by increased uncertainty in dense

regions and is prone to sampling limitations.[50] Conversely, compared to deterministic methods, probabilistic methods have higher computational requirements and are more time-consuming. They are also more sensitive to non-dominant fiber pathways and more likely to produce false positives.[51] Secondly, the definition of nodes is based on the AAL template. Wang et al[52] depicted that different segmentation strategies may affect the topological properties of brain networks. Thirdly, there are differences in disease duration among the EHT group. McEvoy et al[53] suggested that the duration of hypertension is crucial for imaging outcomes. Additionally, some patients in the study were already on antihypertensive medication, and this could potentially influence the topological properties of the brain. Fourthly, the study involved patients with primary hypertension who were cognitively normal and asymptomatic. However, the analysis of the association with dementia was not conducted, as this study primarily adopted a cross-sectional design. To comprehensively comprehend the causal relationship between the variables, additional longitudinal studies are required. Lastly, given the limited sample size in this study, further confirmation is required in larger samples.

Conclusion

In this study, structural networks were constructed using deterministic fiber tracking based on FA values. Moreover, the graph theory approach was utilized to analyze the whole brain network characteristics and intracerebral node characteristics of the two groups. The study revealed a significant increase in AUC values of σ in the EHT group, along with a decrease in AUC values of assortativity. The acquired data indicated the presence of brain network separation and integration dysfunction, mainly in the prefrontal region. Additionally, weight and BMI were positively correlated with σ. These results offer a pathological and physiological foundation for further understanding the impact of EHT on brain networks.

Acknowledgments

This work was partially supported by the Dongguan Science and Technology of Social Development Program (Grant No. 20211800905012). We thank Zhiyun for their linguistic assistance.

Disclosure

The authors report no conflicts of interest in this work.

References

1. World Health Organization. *Global Status Report on the Public Health Response to Dementia 2017–2025*. Geneva: World Health Organization; 2021:27.
2. Sikkes SAM, Tang Y, Jutten RJ, et al. Toward a theory-based specification of non-pharmacological treatments in aging and dementia: focused reviews and methodological recommendations. *Alzheimer's Dis*. 2021;17(2):255–270. doi:10.1002/alz.12188
3. Jones EA, Jenkins B, Addison C2023 Alzheimer's disease facts and figures. *Alzheimer's Dis*. 2023;19(4):1598–1695.
4. Jia P, Lee HWY, Chan JYC, Yiu KKL, Tsoi KKF. Long-term blood pressure variability increases risks of dementia and cognitive decline: a meta-analysis of longitudinal studies. *Hypertension*. 2021;78(4):996–1004. doi:10.1161/HYPERTENSIONAHA.121.17788
5. Sepe-Monti M, Pantano P, Vanacore N, et al. Vascular risk factors and white matter hyperintensities in patients with amnestic mild cognitive impairment. *Acta Neurol Scand*. 2007;115(6):419–424. doi:10.1111/j.1600-0404.2007.00825.x
6. Jellinger KA, Attems J. Prevalence of dementia disorders in the oldest-old: an autopsy study. *Acta Neuropathol*. 2010;119(4):421–433. doi:10.1007/s00401-010-0654-5
7. Faraco G, Iadecola C. Hypertension: a harbinger of stroke and dementia. *Hypertension*. 2013;62(5):810–817. doi:10.1161/HYPERTENSIONAHA.113.01063
8. Li X, Ma C, Zhang J, et al. Prevalence of and potential risk factors for mild cognitive impairment in community-dwelling residents of Beijing. *J Am Geriatr Soc*. 2013;61(12):2111–2119. doi:10.1111/jgs.12552
9. Hughes D, Judge C, Murphy R, et al. Association of blood pressure lowering with incident dementia or cognitive impairment: a systematic review and meta-analysis. *JAMA*. 2020;323(19):1934. doi:10.1001/jama.2020.4249
10. Canavan M, O'Donnell MJ. Hypertension and cognitive impairment: a review of mechanisms and key concepts. *Front Neurol*. 2022;13:821135. doi:10.3389/fneur.2022.821135
11. Douaud G, Menke RA, Gass A, et al. Brain microstructure reveals early abnormalities more than two years prior to clinical progression from mild cognitive impairment to Alzheimer's disease. *J Neurosci*. 2013;33(5):2147–2155. doi:10.1523/JNEUROSCI.4437-12.2013
12. Hannawi Y, Yanek LR, Kral BG, et al. Hypertension is associated with white matter disruption in apparently healthy middle-aged individuals. *Am J Neuroradiol*. 2018;39(12):2243–2248. doi:10.3174/ajnr.A5871
13. Hannesdottir K, Nitkunan A, Charlton RA, Barrick TR, MacGregor GA, Markus HS. Cognitive impairment and white matter damage in hypertension: a pilot study. *Acta Neurol Scand*. 2009;119(4):261–268. doi:10.1111/j.1600-0404.2008.01098.x

14. Chetouani A, Chawki MB, Hossu G, et al. Cross-sectional variations of white and grey matter in older hypertensive patients with subjective memory complaints. *Neuroimage Clin*. 2018;17:804–810. doi:10.1016/j.nicl.2017.12.024
15. Carnevale L, Maffei A, Landolfi A, Grillea G, Carnevale D, Lembo G. Brain functional magnetic resonance imaging highlights altered connections and functional networks in patients with hypertension. *Hypertension*. 2020;76(5):1480–1490. doi:10.1161/HYPERTENSIONAHA.120.15296
16. Unger T, Borghi C, Charchar F, et al. 2020 international society of hypertension global hypertension practice guidelines. *J Hypertens*. 2020;38 (6):982–1004. doi:10.1097/HJH.0000000000002453
17. Cui Z, Zhong S, Xu P, He Y, Gong G. PANDA: a pipeline toolbox for analyzing brain diffusion images. *Front Hum Neurosci*. 2013;7:42. doi:10.3389/fnhum.2013.00042
18. Qian L, Wang Y, Chu K, et al. Alterations in hub organization in the white matter structural network in toddlers with autism spectrum disorder: a 2-year follow-up study. *Autism Res*. 2018;11(9):1218–1228. doi:10.1002/aur.1983
19. Tuch DS, Wedeen VJ, Dale AM, George JS, Belliveau JW. Conductivity tensor mapping of the human brain using diffusion tensor MRI. *Proc Natl Acad Sci USA*. 2001;98(20):11697–11701. doi:10.1073/pnas.171473898
20. Cai Y, Zhao J, Wang L, Xie Y, Fan X. Altered topological properties of white matter structural network in adults with autism spectrum disorder. *Asian J Psychiatr*. 2022;75:103211. doi:10.1016/j.ajp.2022.103211
21. Wang J, Wang X, Xia M, Liao X, Evans A, He Y. GRETNA: a graph theoretical network analysis toolbox for imaging connectomics. *Front Hum Neurosci*. 2015;9:386. doi:10.3389/fnhum.2015.00386
22. Rubinov M, Sporns O. Complex network measures of brain connectivity: uses and interpretations. *Neuroimage*. 2010;52(3):1059–1069. doi:10.1016/j.neuroimage.2009.10.003
23. Watts DJ, Strogatz SH. Collective dynamics of 'small-world' networks. *Nature*. 1998;393(6684):440–442. doi:10.1038/30918
24. Bassett DS, Bullmore ET. Small-world brain networks revisited. *Neuroscientist*. 2017;23(5):499–516. doi:10.1177/1073858416667720
25. Gong G, He Y, Concha L, et al. Mapping anatomical connectivity patterns of human cerebral cortex using in vivo diffusion tensor imaging tractography. *Cereb Cortex*. 2009;19(3):524–536. doi:10.1093/cercor/bhn102
26. Sierra C. Essential hypertension, cerebral white matter pathology and ischemic stroke. *Curr. Med. Chem.* 2014;21(19):2156–2164. doi:10.2174/092986732166613122715514O
27. Pantoni L. Cerebral small vessel disease: from pathogenesis and clinical characteristics to therapeutic challenges. *Lancet Neurol*. 2010;9 (7):689–701. doi:10.1016/S1474-4422(10)70104-6
28. Godin O, Tzourio C, Maillard P, Mazoyer B, Dufouil C. Antihypertensive treatment and change in blood pressure are associated with the progression of white matter lesion volumes: the three-city (3C)-dijon magnetic resonance imaging study. *Circulation*. 2011;123(3):266–273. doi:10.1161/CIRCULATIONAHA.110.961052
29. Morotti A, Shoamanesh A, Oliveira-Filho J, et al. White matter hyperintensities and blood pressure lowering in acute intracerebral hemorrhage: a secondary analysis of the ATACH-2 trial. *Neurocritical Care*. 2020;32(1):180–186. doi:10.1007/s12028-019-00761-0
30. Henskens LH, van Oostenbrugge RJ, Kroon AA, Hofman PA, Lodder J, de Leeuw PW. Detection of silent cerebrovascular disease refines risk stratification of hypertensive patients. *J Hypertens*. 2009;27(4):846–853. doi:10.1097/HJH.0b013e3283232c96
31. Chen Y, Wang Y, Song Z, Fan Y, Gao T, Tang X. Abnormal white matter changes in Alzheimer's disease based on diffusion tensor imaging: a systematic review. *Ageing Res Rev*. 2023;87:101911. doi:10.1016/j.arr.2023.101911
32. Carey RM, Muntner P, Bosworth HB, Whelton PK. Prevention and control of hypertension: jacc health promotion series. *J Am Coll Cardiol*. 2018;72(11):1278–1293. doi:10.1016/j.jacc.2018.07.008
33. Nuttall FQ. Body mass index: obesity, BMI, and health: a critical review. *Nutr Today*. 2015;50(3):117–128. doi:10.1097/NT.0000000000000092
34. Hall JE. The kidney, hypertension, and obesity. *Hypertension*. 2003;41(3 Pt 2):625–633. doi:10.1161/01.HYP.0000052314.95497.78
35. Ahmed SB, Fisher ND, Stevanovic R, Hollenberg NK. Body mass index and angiotensin-dependent control of the renal circulation in healthy humans. *Hypertension*. 2005;46(6):1316–1320. doi:10.1161/01.HYP.0000190819.07663.da
36. Sabisz A, Naumczyk P, Marcinkowska A, et al. Aging and hypertension - independent or intertwined white matter impairing factors? Insights from the quantitative diffusion Tensor imaging. *Front Aging Neurosci*. 2019;11:35. doi:10.3389/fnagi.2019.00035
37. Wang X, Zhao F, Yan S, et al. Role of the prefrontal lobe in young normotensives with a family history of hypertension and hypertensives. *Pflugers Arch*. 2019;471(11–12):1397–1406. doi:10.1007/s00424-019-02313-z
38. Raz N, Rodrigue KM, Acker JD. Hypertension and the brain: vulnerability of the prefrontal regions and executive functions. *Behav Neurosci*. 2003;117(6):1169–1180. doi:10.1037/0735-7044.117.6.1169
39. Bu L, Huo C, Xu G, et al. Alteration in brain functional and effective connectivity in subjects with hypertension. *Front Physiol*. 2018;9:669. doi:10.3389/fphys.2018.00669
40. Friedman NP, Robbins TW. The role of prefrontal cortex in cognitive control and executive function. *Neuropsychopharmacology*. 2022;47 (1):72–89. doi:10.1038/s41386-021-01132-0
41. Wong SW, Massé N, Kimmerly DS, Menon RS, Shoemaker JK. Ventral medial prefrontal cortex and cardiovagal control in conscious humans. *Neuroimage*. 2007;35(2):698–708. doi:10.1016/j.neuroimage.2006.12.027
42. Wang X, Liu B, Xie L, Yu X, Li M, Zhang J. Cerebral and neural regulation of cardiovascular activity during mental stress. *Biomed. Eng. Online*. 2016;15(Suppl 2):160. doi:10.1186/s12938-016-0255-1
43. Norton KN, Luchyshyn TA, Kevin Shoemaker J. Evidence for a medial prefrontal cortex-hippocampal axis associated with heart rate control in conscious humans. *Brain Res*. 2013;1538:104–115. doi:10.1016/j.brainres.2013.09.032
44. Jones DT, Executive G-RJ. Dysfunction and the Prefrontal Cortex. *Continuum*. 2021;27(6):1586–1601. doi:10.1212/CON.0000000000001009
45. Buckner RL, DiNicola LM. The brain's default network: updated anatomy, physiology and evolving insights. *Nat Rev Neurosci*. 2019;20 (10):593–608. doi:10.1038/s41583-019-0212-7
46. Krmpotich TD, Tregellas JR, Thompson LL, Banich MT, Klenk AM, Tanabe JL. Resting-state activity in the left executive control network is associated with behavioral approach and is increased in substance dependence. *Drug Alcohol Depend*. 2013;129(1–2):1–7. doi:10.1016/j.drugalcdep.2013.01.021
47. Feng M, Zhang Y, Liu Y, et al. White matter structural network analysis to differentiate alzheimer's disease and subcortical ischemic vascular dementia. *Front Aging Neurosci*. 2021;13:650377. doi:10.3389/fnagi.2021.650377

48. Zdanovskis N, Platkājis A, Kostiks A, Karelis G, Grigorjeva O. Brain structural connectivity differences in patients with normal cognition and cognitive impairment. *Brain Sci*. 2021;11(7):7. doi:10.3390/brainsci11070943
49. Knösche TR, Anwander A, Liptrot M, Dyrby TB. Validation of tractography: comparison with manganese tracing. *Human Brain Mapp*. 2015;36 (10):4116–4134. doi:10.1002/hbm.22902
50. Avecillas-Chasin JM, Alonso-Frech F, Parras O, Del Prado N, Barcia JA. Assessment of a method to determine deep brain stimulation targets using deterministic tractography in a navigation system. *Neuro Review*. 2015;38(4):739–750. doi:10.1007/s10143-015-0643-1
51. Johansen-Berg H, Gutman DA, Behrens TE, et al. Anatomical connectivity of the subgenual cingulate region targeted with deep brain stimulation for treatment-resistant depression. *Cereb Cortex*. 2008;18(6):1374–1383. doi:10.1093/cercor/bhm167
52. Wang J, Wang L, Zang Y, et al. Parcellation-dependent small-world brain functional networks: a resting-state fMRI study. *Human Brain Mapp*. 2009;30(5):1511–1523. doi:10.1002/hbm.20623
53. McEvoy LK, Fennema-Notestine C, Eyler LT, et al. Hypertension-related alterations in white matter microstructure detectable in middle age. *Hypertension*. 2015;66(2):317–323. doi:10.1161/HYPERTENSIONAHA.115.0533